BOLLETTINO DI GEOFISICA TEORICA ED APPLICATA VOL. 40, N. 3-4, pp. 421-426; SEP.-DEC. 1999

Roughness of the gravity and seafloor topography used to infer geodynamic settings

D. DREHER [(1)], M. F. LALANCETTE [(2)] and M. MAIA[(1)]

[(1)]*UMR 6538 "Domaines océaniques", I.U.E.M., Technopole Brest-Iroise, Plouzane, France*
[(2)]*E.P.S.H.O.M., section Géodésie-Géophysique, Brest Cedex, France*

(Received October 4, 1998; accepted August 5, 1999)

Abstract. In order to systematically study the relationship between gravity and seafloor topography, we have developed a two-dimensional method for calculating the roughness of geophysical data. Roughness is obtained from the energy level of the data within specified wavebands. It is a representation of the spatial distribution of the frequency content of the studied signal. We assume that geodynamic provinces are areas where the gravity and the topography have a homogeneous frequency content.The comparative study of the roughness of both signals consequently allows us to distinguish areas which are situated in a precise geodynamic state. We have chosen characteristic areas of the Eastern North-Atlantic to show how roughness maps of the free air anomaly and the bathymetry signal can be used to infer geodynamic settings. For most of the areas, we find wide homogeneous provinces for both signals which coincide with the dominant geological features (Azores hot spot and mid-Atlantic ridge). In contrast, along the iberian margin, differences of the distribution of roughness maxima between gravity and bathymetry signals suggest different compensation mechanisms.

1. Introduction

We discuss how roughness of free air anomaly and seafloor topography can be used to infer geodynamic settings. As various compensation mechanisms can occur, bathymetry cannot be uniquely recovered from gravity data. The Airy hypothesis appears to be valid for, among other places near-axis seamounts and aseismic ridges, while the Pratt hypothesis appears to hold for long wavelength variations of the gravity data, e.g. thermal subsidence (Gibert and Courtillot, 1987). The Airy model is a limit case of the plate model, which approximates the lithosphere as a thin elastic plate which bends in response to the load. This hypothesis is widely used to analyze compensation for small localized topographic features like intraplate seamounts. Another limit case of that model, considering the elastic

Corresponding author: S. Dreher; UMR 6538 “Domaines oceaniques”, Université de Bretagne Occidentale, I.U.E.M., Technopole Brest-Iroise, 29280 Plouzane, France; phone: +322 98498747; fax: +332 986998760; e-mail: dreher@univ-brest.fr

thickness as being infinite, is the uncompensated model. This model accounts for small wavelength (< 100km) topography to gravity ratios observed in the Atlantic Ocean (McKenzie and Bowin, 1976).

Joint studies in gravity and topography usually consist in determining the compensation depth or the elastic thickness. This latter parameter gives information about the thermal and dynamic setting of the area. A few studies also consider crust and mantle density variations. Estimations of all these parameters, using admittance and coherence, nevertheless require that the geological properties and the geodynamic setting remain uniform in the study area. We therefore used two-dimensional roughness maps of both signals to define boundaries of homogeneous provinces, similarly to a one-dimensional approach presented by Fox and Hayes (1985) for topography. Supposing that an area situated in a precise thermal and/or dynamic setting contains similar topographic features with uniform wavelengths, those homogeneous areas can be considered as areas with an uniform geodynamic setting. This delineation of geographic provinces of limited statistical heterogeneity would also ensure validity for the statistics and spectral analyses which will be carried out later.

2. Two-dimensional roughness

Roughness is generally considered as being the short wavelength content of data which remains after having substracted a general trend to the data (deterministic part). In this work, we consider that roughness represents the spatial distribution of amplitude for a given frequency passband. It therefore characterizes the energy of the frequency content of a signal. To allow the roughness to be described as a function of spatial frequency, we first bandpass filtered the data in 9 frequency bands between 30 and 1000 km. This subdivision has been chosen so as to have a trade off between precision in the frequency domain and computation time. The two-dimensional energy envelope is then computed for each frequency band and normalized in order to be able to compare the different gravity and topography roughness maps.

To filter the data, we used two-dimensional isotropic Butterworth filters of variable order (Shanks, 1967; Kanasewich, 1981). This filter has prooved to be well adapted for this type of study (Gibert et al., 1989; Maia and Diament, 1991), since it has a relatively smooth shape and sharp cutoffs. This ensures a rapid attenuation of the energy outside the waveband. The gain of a band-pass Butterworth filter is

Table 1 - List of pass-bands for the 9 Butterworth filters used for free air anomaly filtering. Cutoff frequencies are indicated for the 99% pass-level recovery and fot the 3 -dB values (50% fall off).

Filter	Order	Pass band at -3 dB (*km*)	Pass band at 99% (*km*)	Compensation mechanism
1	20	27 - 55	30 - 50	uncompensated
2	22	45 - 76	50 - 70	(McKenzie and Bowin, 1976)
3	24	63 - 110	70 - 100	
4	20	90 - 167	100 - 150	regional (elastic flexure)
5	18	134 - 283	150 - 250	(Gilbert and Courillot, 1987)
6	20	224 - 390	250 - 350	
7	13	292 - 600	350 - 500	Pratt
8	14	425 - 825	500 - 700	(Gilbert and Curtillot, 1987)
9	13	590 - 1200	700 - 1000	deep density anomalies (Diament, 1987)

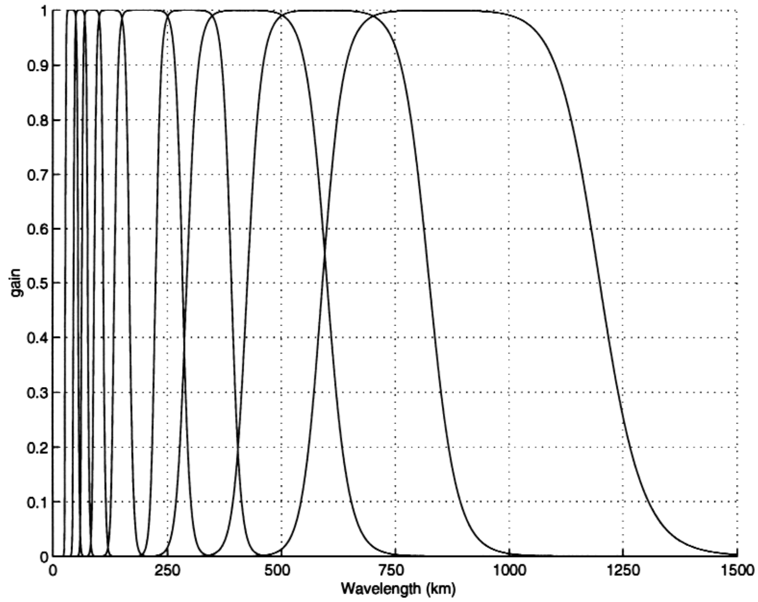

Fig. 1 - Frequency response of the bank of Butterworth filters used to filter the data.

given by:

$$|G(u)|^2 = \left[\frac{1}{1+\left(\frac{u}{u_h}\right)^{2n}} \right] \left[\frac{\left(\frac{n}{n_b}\right)^{2n}}{1+\left(\frac{u}{u_b}\right)^{2n}} \right] \qquad (1)$$

where n is the order of the filter and $[u_b; u_h]$ the passband. u_b and u_h are the cutoff frequencies which are defined by $|G(u_b)^2| = |G(u_h)^2| = 1/2$ and corresponding to the frequencies for which the attenuation is of -3 *dB*.

The two-dimensional version is obtained by replacing the frequency u by the radial frequency

$$u_r = \sqrt{u_x^2 + u_y^2} \ .$$

The frequency response of the bank of filters is represented in Fig. 1. Cutoff frequencies have first been chosen in order to have equispaced frequency bands that intersect at their 99% energy pass level. This ensures a complete coverage of the total waveband (30-1000 km). Some wavebands have then been adapted to fit wavebands related to compensation mechanisms and which have been defined in previous studies (McKenzie and Bowin, 1976; Gibert and Courtillot, 1987; Diament, 1987; Maia and Diament, 1991).

The cutoff frequencies of the filters are presented in Table 1. Limit frequencies for the unity passband are also indicated. The orders of the 9 filters have been chosen to have similar attenuations of about 95 db/octave. The energy envelope of each band-pass filtered signal is obtained from the analytic signal. If *f* is an harmonic function (Nabighian, 1972,1984)

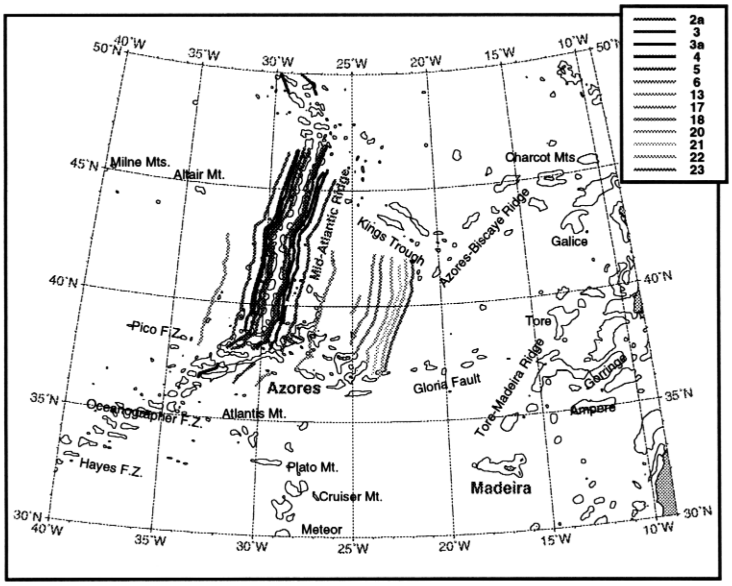

Fig. 2 - Main topographic features of the study area (eastern north-Atlantic) and main magnetic anomalies (compiled by Luis (1996)).

$$\hat{f}(x,y) = \frac{\partial f}{\partial x} + \frac{\partial f}{\partial y} + i\frac{\partial f}{\partial z} \qquad (2)$$

After Roest et al. (1992), the energy envelope is given by $|\hat{f}(x, y)|$. Partial derivatives can be calculated directly in the frequency domain

The roughness maps for both signals can be interpreted separately in order to determine the wavebands in which each characteristic feature of the study area has a signature. To obtain information about the different geodynamic settings, a joint study of gravity and topography roughness must be carried out. Comparing the roughness of bathymetry and gravity data in a particular waveband actually gives an insight into the spatial distribution of the local compensation mode and intensity inside the area.

3. The study area

The method has been applied to a huge area of the eastern part of the North Atlantic Ocean extending from 40° to 9° W and from 30° to 50° N (Fig. 2). As the area is large, wavelengths corresponding to deep geodynamic processes be taken into account. The area contains typical topographic features of the seafloor such as the mid-ocean ridge, abyssal plains, the Iberian margin, seamounts and the Azores hot-spot area. These features correspond to different geodynamic settings and should therefore have different signatures on the roughness maps.

Free-air anomaly data used, come from Sandwell and Smith (1997) and topography data is taken from the General Bathymetric Chart of the Ocean (GEBCO) with some additional data from the EPSHOM (French Naval Hydrographic and Oceanographic Service). Both signals were projected in Transverse Mercator with a 3 km spacing.

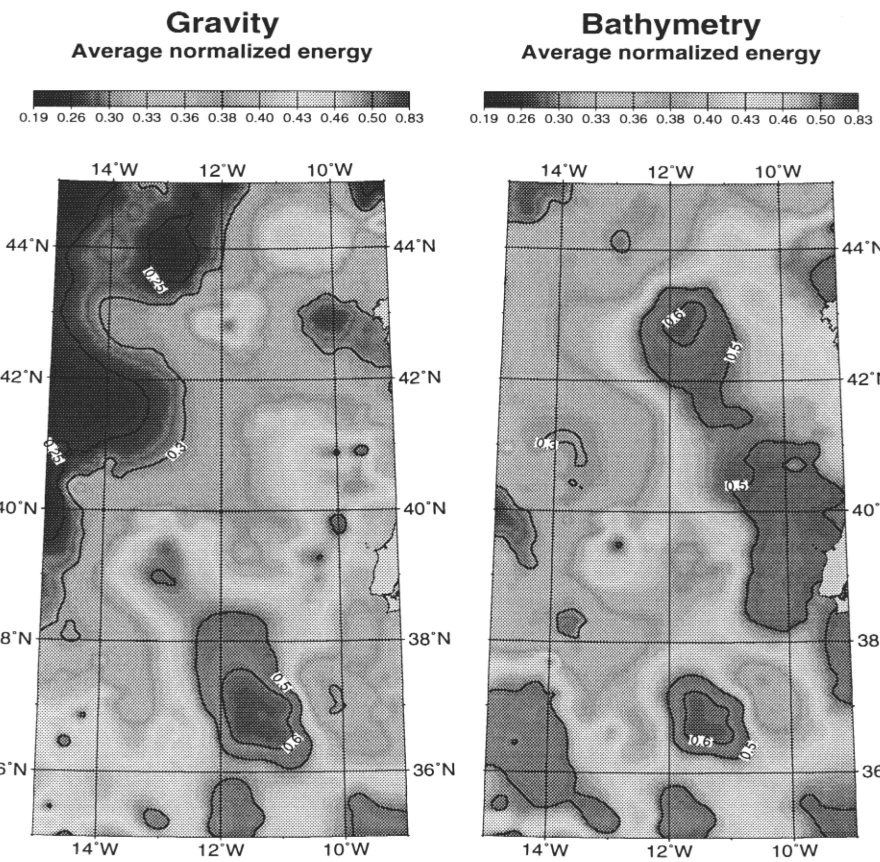

Fig. 3 - Comparative average normalized roughness map of the Gorringe and Galicia bank area. Roughness has been normalized for each waveband and averaged. Differences in the extension and intensity of the roughness between gravity and topography data are clearly visible. Roughness is higher fot the topography in the Galicia bank area. Variations of the characteristics of the compensation mechanisms can account for these differences between the North and the South.

4. Results

The main results are the following:

1. for the first four wavebands, roughness maps of the gravity are very similar to those of the topography. This confirms previous studies which have shown high coherence between both signals below 150 km. Above 150 km, positions of roughness maxima and extension are different for the gravity and topography;
2. the area extending from the Gorringe bank to the Galicia bank has a high roughness in each waveband. Differences of roughness values for the free-air anomaly and the topography are observed between the north and the south of this area (see Fig. 3), suggesting differences in the compensation mechanisms;
3. the mid-Atlantic ridge and the Kings Trough feature are clearly visible in the first three wavebands. The ridge nearly disappears, in the fourth waveband, while the eastern part of the Kings Trough still has a strong signature;

4. in the first four wavebands, localized roughness highs are situated at the locations of the Azores islands. We observe only one roughness maxima which is situated above São Miguel Island for wavebands 5 to 7;
5. in a similar way, for the first three wavebands, roughness highs are situated in correspondence to the seamounts south of the Azores (Plato Mt and Cruiser Mt). For higher wavebands, a large high roughness area containing these seamounts contrasts with the adjacent abyssal plain. In the wavebands above 5, for both the Azores plateau and the southern seamounts area, roughness is higher for the topography than for the gravity.

It appears that all the features described above have a distinct characteristic roughness signature across the bank of wavebands. Various studies of this highly active region showed that those features are marks of the past and present dynamic evolution of the tectonic plates, except for the Azores plateau which is clearly related to a present abnormal behaviour of the mid-Atlantic ridge (Olivet, 1996). The different roughness signature may be related to the fact that they formed in different environments (e.g., compressional environment for the Gorringe bank area, hot-spot environment for the Azores, extensional and strike-slip environment for King's Trough).

References

Diament M.; 1987: *Isostasie, réponses mécanique et thermique de la lithosphère. Application à la géodynamique*. Thèse de Doctorat d'Etat. Thèse nouveau régime, Univ. Paris Sud, Orsay, France.

Fox C. G. and Hayes D. E.; 1985: *Quantitative Methods for Analyzing the Roughness of the Seafloor.* Reviews of Geophysics, **23**, n. 1, 1-48.

Gibert D. and Courtillot V.; 1987: *Seasat altimetry and the south atlantic geoid 1. Spectral analysis.* J. Geophys. Res., **92**, B7, 6235-6248.

Gibert D., Courtillot V. and Olivet J. L.; 1989: *Seasat altimetry and the south atlantic geoid 2. short-wavelength undulations.* J. Geophys. Res., **89**, 5545-5559.

Kanasewich E. R.; 1981: *Time sequence analysis in geophysics.* University of Alberta Press, Edmonton.

Luis J.; 1996: *Le plateau des Agores et le point triple associé: Analyse géophysique et évolution.* Thèse de Doctorat, Univ. Paris VII, France.

Maia M. and Diament M.; 1991: *An analysis of the altimetric geoid in various wavebands in the central pacific ocean: constraints on the origin of intraplate features*. Tectonophys., **190**, 8705-8722.

McKenzie D. and Bowin C.; 1976: *The relationship between bathymetry and gravity in the atlantic ocean.* J. Geophys. Res., **81**, 1903-1915.

Nabighian M. N.; 1972: *The analytic signal of two-dimensional magnetic bodies with polygonal cross-section: Its properties and use for automated anomaly interpretation.* Geophysics, **37**, 3, 507-517.

Nabighian M. N.; 1984: *Toward the tree-dimensional automatic interpretation of potential field data via generalized hilbert transforms: Fundamental relations.* Geophysics, **53**, 957-966.

Olivet J. L.; 1996: *La cinématique de la plaque ibérique [kinematics of the iberian plate].* Bull. Centres Rech. Explor., Prod. Elf Aquitaine, **20**, 1, 131-195.

Roest W. E., Verhoef J. and Pilkington M.; 1992: *Magnetic interpretation using 3-d analytic signal*. Geophysics, **57**, 507-517.

Sandwell D. T. and Smith W. H. F.; 1997: *Marine gravity anomaly from geosat and ers 1 satellite altimetry.* J. Geophys. Res., **102**, B5, 10 039-10 054.

Shanks J. L.; 1967: *Recursion filters for digital processing*. Geophysics, **32**, 33-51.